

Solubility of Sickle Hemoglobin Measured by a Kinetic Micromethod

Dan Liao,* Jose Javier Martin de Llano,[‡] Juha-Pekka Himanen,[‡] James M. Manning,[‡] and Frank A. Ferrone*

*Department of Physics and Atmospheric Science, Drexel University, Philadelphia, Pennsylvania 19104, and [‡]The Rockefeller University, New York, New York 10021 USA

ABSTRACT We have developed a photolytic method to determine the concentration of reactive hemes in a solution in the presence of a trace amount of CO. By measurement of the bimolecular rate of CO binding, and by calibration of the rate constant under equivalent conditions, the concentration of the reactive hemes can be determined. In a solution of sickle hemoglobin, the molecules in the gel contribute negligibly to the recombination rate, allowing the concentration of the molecules in the solution phase to be determined. To optimize signal to noise, modulated excitation methods were employed, although the method could also be used with pulse techniques and suitable signal averaging. Because the optical method employs a microspectrophotometer, only a few microliters of concentrated Hb solution is required to reproduce the entire temperature dependence of the solubility previously determined by centrifugation using milliliter quantities of solutions of the same concentration. This should be especially useful for studies of site-directed mutants, and we present results obtained on one such HbS in which Leu 88 β has been replaced by Ala. The free energy difference in the polymerization of the Leu 88 β double mutant is consistent with known differences in the amino acid hydrophobicities. The calibration required for these experiments also provides an excellent determination of the activation energy for binding the first CO to deoxy Hb.

INTRODUCTION

The gelation of sickle hemoglobin (HbS) involves a phase transition between a monomer phase and a gel phase formed by entangled and weakly cross-linked polymers. Because the polymers reversibly dissociate upon dilution, study of the structure of the polymers has proved challenging. Isolated fibers reveal a 14-strand helical structure (Dykes et al., 1979, Carragher et al., 1988). Crystallography of deoxyHbS has revealed a double-strand pattern (Wishner et al., 1975; Padlan and Love, 1985), which can be transformed into the seven-double strand twisted fiber that is observed in electron microscopy (Watowich et al., 1989). However, because a direct fiber structure does not exist at atomic resolution, the exact placement of the double strands in the fiber is a subject of controversy (Cretgny and Edelstein, 1993; Watowich et al., 1993). In addition, the formation of polymers typically involves a heterogeneous nucleation step (Ferrone et al., 1985a), which by its nature entails contacts between the fibers themselves, and despite its importance has not been explored in structural terms.

Given this state of uncertainty in the fundamental structure, the correlation of structure-function relationships suffers as well. Natural mutants have been helpful in allowing contact sites in the polymer to be identified (Benesch et al., 1982; Nagel and Bookchin, 1978), and this has lent strong support to the hypothesis that the crystal double strands participate in the 14-stranded fiber (Watowich et al., 1989).

With the advent of site-directed mutagenic techniques, new vistas open for the study of structure function relationships in sickle hemoglobin. Perhaps the most fundamental piece of information that can be obtained from such mutants is the solubility. With mutagenic techniques, a premium is placed on the use of small amounts of material. One approach is to employ high-phosphate buffers in which the solubility is sufficiently reduced that the concentration required to produce polymerization is significantly smaller than in lower phosphate buffers (Adachi and Asakura, 1979). However, the possibility remains that the high concentration of phosphate ions will be a confounding variable in understanding the variation between wild-type sickle hemoglobin and a given mutant, even once a proper accounting is made of the effects on sickle hemoglobin itself.

The classic means of determining solubility is to centrifuge a gel and measure the concentration of hemoglobin in the supernatant (Hofrichter et al., 1976). Another approach is to perform a series of measurements of the final amplitude of signals such as turbidity or light scattering at different initial concentrations and extrapolate the amplitudes of the signal to zero. This assumes linearity of the signal, of course. Other so-called scanning methods involve continuous variation of a property that induces gelation, such as temperature or concentration (changed by drying). A well-known example of the latter is measurement of the minimum gelling concentration (MGC) (Bookchin and Nagel, 1971). One variant of the scanning methods involves the change in the oxygen concentration, i.e., the measurement of an oxygen binding curve at a variety of initial concentrations (Benesch et al., 1978). These methods have been extensively compared previously (Sunshine et al., 1979).

In this paper we present a kinetic method that can be used to determine the solubility. Because it is done with microscopic optics it enjoys the advantage of requiring only

Received for publication 17 October 1995 and in final form 16 February 1996.

Address reprint requests to Dr. Frank A. Ferrone, Department of Physics and Atmospheric Science, Drexel University, Philadelphia, PA 19104. Tel.: 215-895-2778; Fax: 215-895-5934; E-mail: frank_ferrone@coasmail.drexel.edu.

© 1996 by the Biophysical Society

0006-3495/96/05/2442/06 \$2.00

micro-samples—typically a few microliters is sufficient. The idea is simply to measure the rate at which a trace amount of CO binds with a solution of HbS. The binding rate should be proportional to the concentration of hemes that can react with the CO, and thus measures the solution phase concentration given that the polymerized hemes are inaccessible or at least have significantly slower binding rates. There are many reasons to expect that the polymer phase will react slowly, and these are discussed later in the paper. As we show, the validity of these assumptions is ensured by the excellent agreement of the data with equilibrium methods employed previously. The implementation of the measurement employs frequency domain measurements, but this is simply a noise reduction strategy. Because no physical separation of the components is involved in the method, it is straightforward to measure the gel under a variety of temperatures for relatively complete thermodynamic characterization with no additional demands on the amount of sample.

In this paper we show in detail how such a method is implemented. (Although this use was suggested previously (Liao et al., 1993), a detailed implementation was not presented.) For completeness we present the theory that underlies the frequency domain method (modulated excitation). Calibration of the method requires measurements on samples of HbA, and this provides a by-product of a precision determination of the activation energy for binding the first CO ligand. We next show the use of the method to obtain the solubility-vs-temperature curve, which essentially reproduces previous work on much larger samples. We conclude by illustrating the use of the technique on a mutant HbS in which a well-known intermolecular contact, $\beta 88$ Leu, has been replaced by an Ala.

THEORY

The method described is a type of modulated excitation (Ferrone, 1994). Consider a sample that has a concentration of hemes c_o , which is divided into singly liganded tetramers, whose heme concentration is S , and deoxy hemes of concentration D . A laser of intensity I is turned on and off sinusoidally with a frequency f (in Hz), which is related to the angular frequency by $\omega = 2\pi f$. The mathematics of the problem are considerably simplified by writing the oscillatory signal as a complex number, whose real and imaginary projections are defined as the oscillations in and out of phase, respectively. Thus the intensity of the laser is given by $I(t) = I(1 + e^{i\omega t})$. The presence of the 1 ensures that the intensity is not negative. (It is also possible to provide a small steady-state beam on top of which the oscillation occurs, which would place a factor before the $e^{i\omega t}$ term.) The rate of dissociation of liganded hemes provided by this beam is the product of the absorbance of the beam, the quantum yield q , and the beam intensity, thus

$$(-dS/dt)_{\text{photo}} = (dD/dt)_{\text{photo}} = 2.3\epsilon zSqI(t), \quad (1)$$

in which ϵ is the extinction coefficient for the liganded species at the laser wavelength, and z is the path length. The 2.3 arises from a $\ln(10)$ term.

The full differential equation for the deoxy population D involves recombination of deoxy hemes with free CO, whose concentration we denote by X . Because only a small amount of CO is present, X will vary with time, as do D and S . Thus

$$dS/dt = -dD/dt = kX(t)D(t) - 2.3\epsilon zS(t)qI(t), \quad (2)$$

where k is the bimolecular rate constant for binding CO to an to an unliganded heme. In an allosteric description this would be labeled k_T . Because $I(t)$ is oscillatory, $S(t)$ and $D(t)$ will oscillate as well. In general,

$$D(t) = \sum_n D_n(\omega)e^{in\omega t}, \quad (3)$$

and a similar equation can be written for $S(t)$.

Because $D(t) + S(t) = c_o$, and because c_o is a constant, the time-dependent parts are negatives of each other, as already used above in the relationship $dS/dt = -dD/dt$. Because the terms in the sum in Eq. 3 are all independent, $D_n = -S_n$. Moreover, the concentration of free ligand will also change because of photodissociation, and $dX/dt = dS/dt$. Because $X(t)$ can be expanded in the same type of equation as Eq. 3, it follows that $X_n = S_n$ ($n > 0$). The $n = 0$ term contains a contribution from the free ligand concentration when no photolysis is active. Substituting gives the equations for $n = 0$ and $n = 1$, viz.,

$$0 = kX_oD_o - 2.3\epsilon zqIS_o, \quad (4a)$$

$$-i\omega D_1 = k(-D_1D_o + X_oD_1) + 2.3\epsilon zqI(D_1 - S_o), \quad (4b)$$

where only $n = 1$ or lower terms are retained in Eq. 4b and the common $e^{i\omega t}$ has been canceled. From Eq. 4b:

$$D_1 = \frac{2.3\epsilon zqIS_o}{k(D_o - X_o) + 2.3\epsilon zqI + i\omega}. \quad (5)$$

Because S_o is typically small ($S_o/D_o < 2\%$), it follows that $c_o \approx D_o$. Then, in the limit where $kc_o \gg 2.3\epsilon zqI$, the first harmonic ($n = 1$) oscillating population of deoxy hemes is

$$D_1 = \frac{2.3\epsilon zqIS_o}{kc_o + i\omega}. \quad (6)$$

The magnitude of the signal is simply

$$|D_1| = \frac{2.3\epsilon zqIS_o}{\sqrt{(kc_o)^2 + \omega^2}}. \quad (7a)$$

The tangent of the phase angle ($\tan \phi$) is defined as the imaginary part of D_1 divided by the real part, and is given by $\tan \phi = -\omega/kc_o$ or

$$kc_o = -\omega \cot \phi. \quad (7b)$$

Thus, when c_o is known, as in the calibration experiment, k can be determined. Conversely, once k is known, c_o can be

determined. The cotangent of phase is determined by measuring the signal amplitude, which oscillates in phase with the laser excitation, and that which oscillates 90° out of phase with the laser oscillation. In the formalism used here, the in-phase part is the real part, whereas the out-of-phase part is the imaginary part. Thus $\cot \phi$ is determined by the in-phase signal divided by the out-of-phase signal.

From Eq. 7a the amplitude of the signal depends on I and S_o . Both of these are constrained to remain small to allow the assumptions of the calculation to retain validity. The laser intensity I must be small enough for $kc_o \gg 2.3\epsilon zqI$. The concentration of liganded hemes S_o must be small enough that there are insignificant numbers of doubly liganded molecules whose recombination rate will differ from k . (This is also important for the solubility measurement, so that the solubility is not affected by the presence of a nonpolymerizing component.) The modulation frequency ω is selected to give a $\cot \phi \approx 1$, thereby making equal signals in the two detected channels. When $\cot \phi \approx 1$, Eq. 7a becomes $|D_1| = 0.7 (2.3\epsilon zqI/kc_o)S_o$. Because of the requirement that $2.3\epsilon zqI/kc_o \ll 1$ as well as $S_o \ll c_o$, the signal is intrinsically weak (on the order of 10^{-4} of c_o) and must be extensively averaged.

MATERIALS AND METHODS

HbS and HbA were purified by standard methods and stored in liquid nitrogen until use (Cho and Ferrone, 1991; Liao et al., 1993). HbS(L88 β A) was prepared and characterized as described elsewhere (Martin de Llano et al., 1993). Solutions were concentrated with Microcon concentrators. Concentrations of HbA were measured using the oxy derivative Soret absorbance. Samples were exchanged into 0.15 M phosphate buffer, pH 7.3 (HbA and S) and pH 7.1 (HbS(L88 β A)).

Concentrated sodium dithionite ($\text{Na}_2\text{S}_2\text{O}_4$) solution (in phosphate buffer) was added to the oxyHb solutions to give a final dithionite concentration of 0.5 to 0.55 M. HbA and HbS were prepared as 10- μl solutions, with 1 μl of appropriately concentrated dithionite added. HbS(L88 β A) was prepared as 4 μl of concentrated protein, to which 1 μl of dithionite solution was added. Dithionite was measured with 1- μl full-scale Hamilton syringes or the equivalent; Hb volumes were measured by micropipette. Dithionite addition was performed in a cold box flushed with nitrogen or a $\text{CO}:\text{N}_2$ mixture (see below.) Samples of sickle hemoglobin were kept on ice until the final step of preparation.

Trace amounts of CO were introduced by using a certified mixture of 100 ppm CO in N_2 (Airco). The CO was added to the samples by flushing a 1-ml vial with the $\text{CO}:\text{N}_2$ mixture for 5 min, into which the Hb was injected, followed by the dithionite. After the addition of dithionite a stream of humidified $\text{CO}:\text{N}_2$ mixture was directed over the sample for an additional 1–2 min. Approximately 2- μl drops of samples were then placed on a 24×50 mm coverslip, promptly covered by a second coverslip (22 mm square), and sealed with Kerr sticky wax in the cold box. Spectrophotometry of the resultant samples did not resolve any remnant of the CO peak on the shoulder of the deoxy Soret peak, limiting the amount of CO in the final solution to $<2\%$. As described below, however, the CO present is sufficient to observe the kinetics needed in the experiment.

Once the sample was prepared, an absorption spectrum was measured. Sample absorbance was kept between 1 and 1.5 OD. After the absorbance measurement, modulated excitation measurements were performed on an apparatus previously described (Ferrone, 1994). Excitation used the 488-nm line from an argon ion laser, reduced with neutral density filters and controlled by an electro-optic modulator system (CRI). As a control measurement, the modulated excitation spectrum of the sample was measured to confirm that the modulated species was HbCO and that no artifacts

were responsible for the modulated signal. Spectra were obtained between 400 and 450 nm. Finally the apparatus was set to 436.5 nm to measure the phase angle relative to the excitation beam.

The temperature was regulated with a Cambion thermoelectric stage and a controller of our own design. The temperature was calibrated by use of a thermistor probe placed in the position of the sample.

The sample area observed was a 0.48 mm square. The laser beam was brought to a spot size that just filled the square. The scattered laser light was blocked from the photodetector by the use of a square mask and glass filter, in addition to the monochromator that was placed before the photomultiplier. AC leakage was verified to be insignificant in the spectral region observed. Laser power was measured by a calibrated pyroelectric detector (Coherent) and digital voltmeter (Keithly). Typical power levels were about 20 mW, which yield a power density at the sample of 11 W/cm^2 . Based on an extensive set of experiments with thin, concentrated samples (Ferrone et al., 1985b), this power density should yield insignificant DC heating ($<1^\circ\text{C}$).

RESULTS

Calibration experiments were performed on two samples of HbA, prepared on different days, of concentration 10.7 mM and 12.3 mM. Each measurement of the cotangent involved signal averaging for about 20 min. The angular frequency ω was $5.05 \times 10^3 \text{ s}^{-1}$. In-phase and out-of-phase signals were averaged separately, and the ratio of the averages was taken. The process was generally performed three times, and the error bars shown reflect the standard deviation of the triplicate set. Measurements were performed at a series of temperatures, and the result is shown in Fig. 1. The two sets of data fall on a single line, with an activation energy of 9.2 kcal/mol.

The experiment was repeated on a sample of HbS of initial concentration 30.8 g/dl (19.2 mM (heme)) at a series

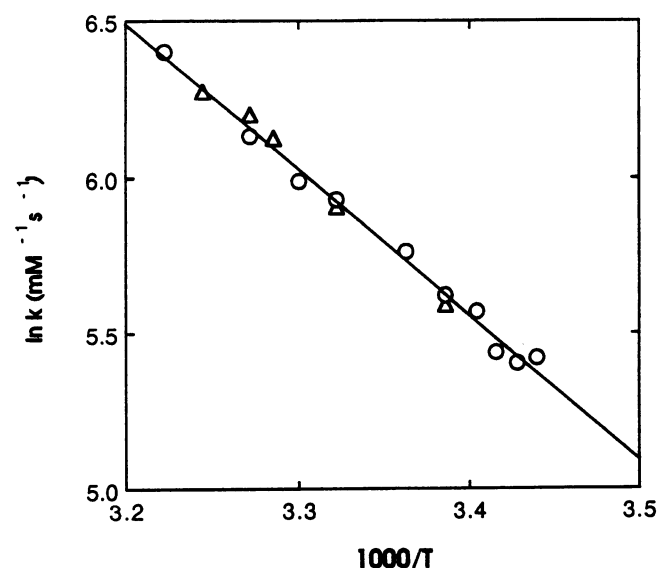


FIGURE 1 Log of the rate constant for binding the first CO to a deoxy-HbA molecule, as a function of reciprocal temperature (K). Rate constants were determined by use of Eq. 7b. $\omega = 5.05 \times 10^3 \text{ s}^{-1}$. Two concentrations are shown: 10.7 mM and 12.3 mM (heme). The activation energy is 9.2 kcal/mol.

of nine temperatures. Despite the fact that the concentration is higher than in the HbA samples, the cotangents give a lower concentration, indicating that the solution phase monomers are being observed. Temperatures were not taken in a monotonic sequence. The concentration of hemes that rebind was determined by using Eq. 7b and dividing by the rate constant k determined from the calibration experiment in Fig. 1. The concentration is shown as a function of temperature in Fig. 2 as the closed symbols.

The open symbols in Fig. 2 show the solubility measurement taken on a sample of HbS(L β 88A). Because of the small amount of Hb available after concentration, an initial concentration measurement was not performed, but the concentration is estimated to be near 35 g/dl. The solubility is clearly higher than pure HbS and shows much less temperature variation.

DISCUSSION

The ability of this method to measure concentration accurately depends critically on the measurement of a calibration set of rate constants. Fig. 1 shows that a consistent set of data can be obtained, which allows for an accurate interpolation of rates.

It is also necessary that the rate of ligand rebinding to the polymer be much less than that in the monomer phase. Although the success of the method argues that the assumptions are justified, it is also possible to justify this assumption by noting previous experiments. Using differential in-

terference contrast microscopy, Briehl has directly observed the growth and melting of sickle hemoglobin fibers induced by photolysis (Briehl, 1995). Extinguishing the photolysis beam permitted recombination with ligand and subsequent melting. Fibers were observed to shrink rather than disintegrate, and the decrease occurred at a much slower rate than the impinging diffusion of CO into the photolyzed volume. This implies that a polymer will take up CO present in the solution around it at a substantially slowed rate. Shapiro, Klinger, and co-workers determined the rate of polymer recombination with CO by measuring kinetic linear dichroism, and their results placed the recombination rate at several orders of magnitude lower than observed in solution, consistent with Briehl's observations (Shapiro et al., 1995). Thus the assumption that the recombination is dominated by solution-phase molecules appears valid.

The solubility of pure HbS under conditions very similar to those used here has been measured previously (Ross et al., 1977); the results are shown as the dashed line in Fig. 2. As can be seen, the agreement is excellent. In the previous method, centrifugation of tubes containing gels was used to physically separate monomers, which were measured as the supernatant concentration. In those experiments each measurement of solubility utilized 360 μ l of solution, which would have required >3 ml of concentrated solution if the pelleted HbS had not been reused. In contrast, the method here has utilized \sim 5 μ l of the same concentration. Whereas each data point, taken in triplicate, takes almost an hour to measure, the centrifugation in the previous method is done for about 3 h.

The solubility of the double mutant HbS β 88A at 37°C is about 29.6 g/dl, which is in reasonable agreement with the single existing measurement of 31.2 g/dl, taken at 37°C (de Llano and Manning, 1994). The latter was determined by a method (Benesch et al., 1978) that involves the measurement of the half-saturation pressure (p_{50}) for various concentrations of Hb. The method uses a scanning oxygenation device (e.g., Hem-O-Scan) and is useful in its ability to estimate the solubility of a small amount of material without recourse to high phosphate buffers. However, there are also a number of limitations in that procedure (Sunshine et al., 1979). As a scanning method, there is a necessary complication due to associated kinetic processes. Although these can be minimized by melting a gel rather than forming a gel, and thereby avoiding the possibility of a long delay time, there is still the issue of oxygen penetration and melting of the gel while the scan proceeds. This effect underestimates the solubility. A second complication is that the method intrinsically measures the solubility in the presence of ligands, which overestimates the solubility. For example, the solubility of HbS at 50% oxygen saturation has been determined to be closer to 22 g/dl than to 17 g/dl (Sunshine et al., 1982). Finally, the theoretical foundations of the method are somewhat uncertain, particularly the origin of the change in p_{50} with concentration even in the absence of a gel. A theoretical description of this process predicts no concentration dependence of the p_{50} below solubility, and a non-

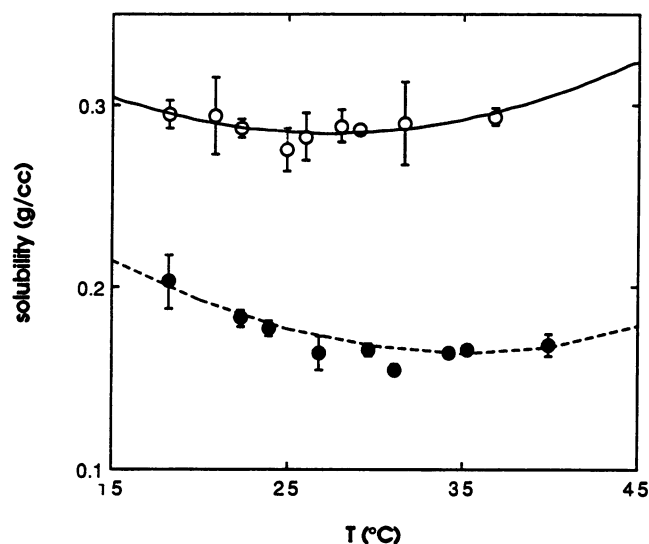


FIGURE 2 Solubility as a function of temperature. The lower curve (filled symbols) gives the solubility of unmodified HbS, and the upper curve (open symbols) gives the result for the double mutant (HbS β 88A). Solubility was determined by using Eq. 7b and the calibrated rate constants shown in Fig. 1. Error bars represent the standard deviation of triplicate measurements. The dashed curve through the unmodified HbS data is the fit described by Eaton and Hofrichter (1990) to the data of Ross et al. (1977). The upper curve is the best fit of a second-order curve: $c_s = 0.38 - 0.0070 T + (1.27 \times 10^{-4})T^2$.

linear behavior above it (Hofrichter, 1979). In a series of non-scanning measurements for HbA, Gros et al. (1978) found no concentration dependence of p_{50} , as expected. Given these considerations, the two determinations of the solubility of HbS $\beta 88A$ must be considered consistent.

From the data of Fig. 2 it is possible to determine the free energy of polymerization. To do so requires two additions to the customary $-RT \ln c_s$. First, nonideality must be taken into account. Second, because the specific volume of hemoglobin in the polymer phase is greater than that in the monomer phase, the activity of water must be considered. Thus the equilibrium constant for the polymerization reaction can be written as

$$K = (\gamma_s c_s)^{-1} a_w^{-1}, \quad (8)$$

where a_w is the activity of the number of moles of water involved in the polymerization reaction (Eaton and Hofrichter, 1990). Thus the free energy can be written as

$$\Delta G = RT \ln K = -RT \ln c_s - RT \ln \gamma_s - RT \ln a_w. \quad (9)$$

The third term is given by

$$-RT \ln a_w = RT \int_0^{c_s(1/c_p) - v} \left(1 + \frac{\partial \ln \gamma}{\partial \ln c} \right) dc, \quad (10)$$

in which c_p is the concentration in the polymer phase, v is the specific volume in the monomer phase, and c is concentration (Eaton and Hofrichter, 1990).

Fig. 3 *a* shows the free energy of polymerization for

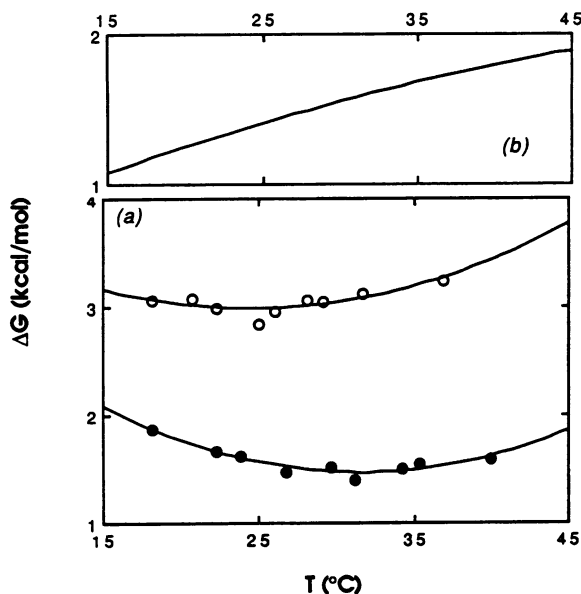


FIGURE 3 (a) Free energy of polymerization as a function of temperature. The data of Fig. 2 have been used in conjunction with Eqs. 9 and 10. Both data sets are fit by second-order curves. The HbS data are best fit by $3.70 - 0.14T + 0.0022T^2$; the HbS($\beta 88A$) data are best fit by $4.14 - 0.094T + 0.00197T^2$. (b) The difference between the two free energies, as determined by their best fits, is shown as a function of temperature, in which it is almost linear.

mutant and HbS. The water correction (Eq. 10) accounts for about 0.2 kcal/mol. The difference between the two curves is shown as Fig. 3 *b*. The difference curve is almost linear in T , as would appear from a totally entropic effect.

The solubility for this mutant Hb has also been measured in 1.8 M phosphate buffers, in which the low solubilities permit study with small amounts of material (Adachi et al., 1995). It is interesting to compare the free energy differences between HbS and HbS($\beta 88A$) in that solvent. To do so, Eq. 9 can be employed without the second and third terms, because in those low concentrations the dilute, ideal limit is appropriate. The difference in assembly free energy due to the replacement of Leu by Ala in high phosphate buffer is about 1 kcal/mol (Adachi et al., 1995), which is similar to but nevertheless different from the effect seen under the buffer system employed here. This suggests that high phosphate buffers have additional specific effects on the contact site and must be used with caution.

The hydrophobic interaction of water with various amino acids has been measured by determining their solubility in ethane versus water. Such a procedure gives a difference of 1.3 kcal/mol at 25°C for the replacement of Ala by Leu (Nozaki and Tanford, 1971). Only one of the two $\beta 88$ sites per tetramer is implicated in intermolecular contacts (Padlan and Love, 1985). Thus the net difference in polymerization free energy is expected to be about 1.3 kcal/mol. Although this standard hydrophobic difference is quite close to the measured difference of about 1.5 kcal/mol, the agreement may be fortuitous, because it is not clear that the entire Ala or Leu should be considered solvated (and hydrophobic interactions roughly scale with accessible surface area.) There is also the question of whether vibrational motions of the monomers within the polymer are affected by this substitution, for if so, they will provide an entropic difference that in turn affects the overall equilibrium and hence the solubility. The exploration of such issues is beyond the scope of solubility measurements alone.

We thank Zhiqi Cao for her assistance in the preparation of the samples.

REFERENCES

- Adachi, K., and T. Asakura. 1979. Nucleation-controlled aggregation of deoxyhemoglobin S. Possible difference in the size of nuclei in different phosphate concentrations. *J. Biol. Chem.* 254:7765-7771.
- Adachi, K., P. Konitzer, G. Paulraj, and S. Surrey. 1995. Role of Leu- $\beta 88$ in the hydrophobic acceptor pocket for Val- $\beta 6$ during hemoglobin S polymerization. *J. Biol. Chem.* In press.
- Benesch, R. E., R. Edalji, S. Kwong, and R. Benesch. 1978. Oxygen affinity as an index of hemoglobin S polymerization: a new micro-method. *Anal. Biochem.* 89:162-173.
- Benesch, R. E., S. Kwong, and R. Benesch. 1982. The effects of α chain mutations *cis* and *trans* to the $\beta 6$ mutation on the polymerization of sickle cell hemoglobin. *Nature.* 299:231-234.
- Bookchin, R. M., and R. L. Nagel. 1971. Ligand induced conformational dependence of hemoglobin in sickling interactions. *J. Mol. Biol.* 60: 263-270.
- Briehl, R. 1995. Nucleation, fiber growth and melting, and domain formation and structure in sickle cell hemoglobin gels. *J. Mol. Biol.* 245: 710-723.

- Carragher, B., D. A. Bluemke, B. Gabriel, M. J. Potel, and R. Josepfs. 1988. Structural analysis of sickle hemoglobin polymers. I. Sickle hemoglobin fibers. *J. Mol. Biol.* 199:315–331.
- Cho, M. R., and F. A. Ferrone. 1991. Monomer diffusion and polymer alignment in domains of sickle hemoglobin. *Biophys. J.* 63:205–214.
- Cretny, I., and S. J. Edelstein. 1993. Double strand packing in hemoglobin S fibers. *J. Mol. Biol.* 230:733–738.
- Dykes, G. W., R. H. Crepeau, and S. J. Edelstein. 1979. Three dimensional reconstruction of 14-filament fibers of hemoglobin S. *J. Mol. Biol.* 130:451–472.
- Eaton, W. A., and J. Hofrichter. 1990. Sickle cell hemoglobin polymerization. *Adv. Protein Chem.* 40:63–280.
- Ferrone, F. A. 1994. Modulated excitation spectroscopy in hemoglobin. *Methods Enzymol.* 232:292–321.
- Ferrone, F. A., J. Hofrichter, and W. A. Eaton. 1985a. Kinetics of sickle hemoglobin polymerization. II. A double nucleation mechanism. *J. Mol. Biol.* 183:611–631.
- Ferrone, F. A., J. Hofrichter, and W. A. Eaton. 1985b. Kinetics of sickle hemoglobin polymerization. I. Studies using temperature-jump and laser photolysis techniques. *J. Mol. Biol.* 183:591–610.
- Gros, G., H. S. Rollema, W. Jelkmann, H. Gros, C. Bauer, and W. Moll. 1978. Net charge and oxygen affinity of human hemoglobin are independent of hemoglobin concentration. *J. Gen. Physiol.* 72:765–773.
- Hofrichter, J. 1979. Ligand binding and the gelation of sickle cell hemoglobin. *J. Mol. Biol.* 128:335–369.
- Hofrichter, J., P. D. Ross, and W. A. Eaton. 1976. Supersaturation in sickle cell hemoglobin solutions. *Proc. Natl. Acad. Sci. USA.* 73:3035–3039.
- Liao, D., J. Jiang, M. Zhao, and F. A. Ferrone. 1993. Modulated excitation of singly ligated carboxyhemoglobin. *Biophys. J.* 65:2059–2067.
- Martin de Llano, J. J., and J. M. Manning. 1994. Properties of a recombinant human hemoglobin double mutant: sickle hemoglobin with Leu-88 β at the primary aggregation site substituted by Ala. *Protein Sci.* 3:1206–1212.
- Martin de Llano, J. J., O. Schneewind, G. Stetler, and J. M. Manning. 1993. Recombinant human sickle hemoglobin expressed in yeast. *Proc. Natl. Acad. Sci. USA.* 90:918–922.
- Nagel, R. L., and R. M. Bookchin. 1978. Areas of intraction in the HbS polymer. In *Biochemical and Clinical Aspects of Hemoglobin Abnormalities*. W. S. Caughey, editor. Academic Press, New York. 195–203.
- Nozaki, Y., and C. Tanford. 1971. The solubility of amino acids and two glycine peptides in aqueous ethanol and dioxane solutions. *J. Biol. Chem.* 246:2211–2217.
- Padlan, E. A., and W. E. Love. 1985. Refined crystal structure of deoxy-hemoglobin S. *J. Biol. Chem.* 260:8280–8291.
- Ross, P. D., J. Hofrichter, and W. A. Eaton. 1977. Thermodynamics of gelation of sickle cell deoxyhemoglobin. *J. Mol. Biol.* 115:111–134.
- Shapiro, D. B., R. M. Esquerra, R. A. Goldbeck, S. K. Ballas, N. Mohandas, and D. Kliger. 1995. Carbon monoxide religation kinetics to hemoglobin S polymers following ligand photolysis. *J. Biol. Chem.* 270:26078–26085.
- Sunshine, H. R., F. A. Ferrone, J. Hofrichter, and W. A. Eaton. 1979. Gelation assays, and the evaluation of therapeutic inhibitors. In *Development of Therapeutic Agents for Sickle Cell Disease*. J. Rosa, Y. Beuzard, and J. Hercules, editors. Elsevier-North Holland, New York. 31–46.
- Sunshine, H. R., J. Hofrichter, F. A. Ferrone, and W. A. Eaton. 1982. Oxygen binding by sickle cell hemoglobin polymers. *J. Mol. Biol.* 158:251–273.
- Watowich, S. J., L. J. Gross, and R. J. Josepfs. 1989. Intramolecular contacts within sickle hemoglobin fibers. *J. Mol. Biol.* 209:821–828.
- Watowich, S. J., L. J. Gross, and R. Josepfs. 1993. Analysis of the intermolecular contacts within sickle hemoglobin fibers: effect of site-specific substitutions, fiber pitch and double-strand disorder. *J. Struct. Biol.* 111:161–179.
- Wishner, B. C., K. B. Ward, E. E. Lattman, and W. E. Love. 1975. Crystal structure of sickle-cell deoxyhemoglobin at 5 Å resolution. *J. Mol. Biol.* 98:179–194.